Available online at www.sciencedirect.com

ScienceDirect

journal homepage: www.elsevier.com/locate/he

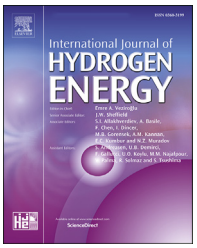

Optimization and modeling of process parameters during hydrothermal gasification of biomass model compounds to generate hydrogen-rich gas products

Jude A. Okolie [a], *Sonil Nanda* [b], *Ajay K. Dalai* [a,*], *Janusz A. Kozinski* [c]

[a] *Department of Chemical and Biological Engineering, University of Saskatchewan, Saskatoon, Saskatchewan, Canada*

[b] *Department of Chemical and Biochemical Engineering, University of Western Ontario, London, Ontario, Canada*

[c] *Department of Chemical Engineering, University of Waterloo, Waterloo, Ontario, Canada*

ARTICLE INFO

Article history:
Received 3 April 2019
Received in revised form
6 May 2019
Accepted 14 May 2019
Available online xxx

Keywords:
Box-Behnken design
Hydrothermal gasification
Hydrogen
Synthetic biomass
Process optimization

ABSTRACT

Hydrothermal gasification in subcritical and supercritical water is gaining attention as an attractive option to produce hydrogen from lignocellulosic biomass. However, for process optimization, it is important to understand the fundamental phenomenon involved in hydrothermal gasification of synthetic biomass or biomass model compounds, namely cellulose, hemicellulose and lignin. In this study, the response surface methodology using the Box-Behnken design was applied for the first time to optimize the process parameters during hydrothermal (subcritical and supercritical water) gasification of cellulose. The process parameters investigated include temperature (300–500 °C), reaction time (30–60 min) and feedstock concentration (10–30 wt%). Temperature was found to be the most significant factor that influenced the yields of hydrogen and total gases. Furthermore, negligible interaction was found between lower temperatures and reaction time while the interaction became dominant at higher temperatures. Hydrogen yield remained at about 0.8 mmol/g with an increase in the reaction time from 30 min to 60 min at the temperature range of 300–400 °C. When the temperature was raised to 500 °C, hydrogen yield started to elevate at longer reaction time. Maximum hydrogen yield of 1.95 mmol/g was obtained from supercritical water gasification of cellulose alone at 500 °C with 12.5 wt% feedstock concentration in 60 min. Using these optimal reaction conditions, a comparative evaluation of the gas yields and product distribution of cellulose, hemicellulose (xylose) and lignin was performed. Among the three model compounds, hydrogen yields increased in the order of lignin (0.73 mmol/g) < cellulose (1.95 mmol/g) < xylose (2.26 mmol/g). Based on the gas yields from these model compounds, a possible reaction pathway of model lignocellulosic biomass decomposition in supercritical water was proposed.

* *Corresponding author.*
E-mail address: ajay.dalai@usask.ca (A.K. Dalai).

https://doi.org/10.1016/j.ijhydene.2019.05.132
0360-3199/

Introduction

Over the past few years, biofuel economy is perceived as one of the most promising alternatives to mitigate the challenges of greenhouse gas emissions and unmatchable reliance on fossil fuels [1]. Hydrogen (H_2) is a clean and efficient energy source, which can be used as a direct fuel or converted into other hydrocarbon fuels and chemicals through Fischer-Tropsch catalysis [2,3]. Since the product of combustion of H_2 is water, its utilization is widely regarded as being environmentally benign. Hydrogen finds many industrial applications in the upgrading of conventional petroleum, production of ammonium and desulfurization of heavy oils to meet stringent environmental regulations [4]. Commercial H_2 is produced from the steam reforming of methane [5,6] due to its low production cost of US$ 1.5–3.7 per kg [7]. Only a small fraction of the global supply of H_2 gas is obtained from electrolysis of water due to the high energy requirement of the process [8]. To reduce the over dependency on fossil fuels such as methane and reduce greenhouse gas emissions, the use of alternative resources for H_2 production such as lignocellulosic biomass is highly plausible.

Non-edible plant residues (i.e. lignocellulosic biomass) are renewable, plentiful and widely regarded as an inexpensive source for renewable energy generation [9–11]. Hydrogen can be produced through several thermochemical and biochemical methods. The thermochemical technologies for H_2 generation include steam reforming, autothermal reforming, partial oxidation, gasification and pyrolysis, whereas the biological technologies involve the participation of photosynthetic microorganisms such as photoheterotrophic bacteria and photoautotrophic algae [12–14]. Subcritical and supercritical water gasification are promising alternatives routes for producing H_2 from high-moisture containing biomass [15].

Supercritical water (SCW) exists at temperatures and pressures beyond the critical point of pure water (374 °C and 22.1 MPa). Biomass is efficiently solubilized in SCW to produce gases consisting of H_2, CO_2, CO, CH_4 and smaller amounts of C_{2+} components [16]. SCW exhibits gas-like viscosity and liquid-like density, which makes it act like a green solvent to dissolve highly recalcitrant organic compounds to permanent gases [17,18]. In addition, there is a significant reduction in the dielectric constant of water under supercritical conditions, which increases its ability to dissolve non-polar compounds [19]. The syngas (H_2 + CO) obtained at high pressures from supercritical water gasification (SCWG) also reduces the compression costs for industrial applications.

Numerous studies have been published on the SCWG of different biomass compounds [20–28]. However, the high heterogeneity and complexity of real biomass compounds still pose a significant challenge for conducting experimental studies to understand the fundamentals of SCWG process and its reaction pathway [29]. Therefore, it is essential to understand the decomposition behavior of individual biomass model compounds (e.g. cellulose, hemicellulose and lignin) and their interactions under supercritical conditions. These model compounds can imitate the composition of real biomass, thereby making it easier to explore the reaction pathways during SCWG [30].

Cellulose, hemicellulose and lignin as the three main functional compounds in lignocellulosic biomass [9]. Extractives, also present as the non-structural components in lignocellulosic biomass, are readily soluble in water or neutral organic solvents. There are a few studies that report SCWG of biomass model compounds such as glucose [31], xylan [32] and lignin [33]. In addition, SCWG of fructose [34] and lactose [35] have also been reported as the model compounds of waste fruits and dairy products. Yoshida and Matsumura [36] examined the combined gasification of cellulose, xylan and lignin mixtures to understand the interactions among the three main constituents of lignocellulosic biomass. They showed that there was no signification interaction between cellulose and xylan. However, the presence of lignin in the feedstock significantly lowered H_2 and total gas yield, which suggested an interaction between lignin and holocellulose (cellulose and hemicellulose).

Despite the vast amount of literature available for the gasification of several biomass in SCW, only a few studies have investigated the decomposition patterns and behavior of the biomass model compounds. Moreover, studies on the effect of experimental conditions (i.e. temperature, reaction time and feedstock concentration) and their interactions on H_2 yield during SCWG is scarce in the literature. A lucid understanding of the effect of different experimental conditions and their interfaces during SCWG could be useful for determining the process economics and optimization. Most studies in SCWG applies the univariate approach to study the influence of experimental conditions. Such procedures involve investigating the effect of a single process parameter while maintaining the other variables constant [33]. Such approaches can discount the interrelated effects among other significant parameters, thereby shedding their actual impacts on gas yields. If these parameters were altered together, and not individually, their combined impacts on syngas yields can be easily elucidated. Statistical models can be applied to study the interaction effects among each parameter. Kang et al. [33] reported a central composite design (CCD) to optimize H_2 yields from non-catalytic gasification of lignin in SCW. At 600 °C, they observed a strong interaction between temperature and water-to-biomass ratio.

In the current work, we investigated the interactions among the process parameters (e.g. temperature, reaction time and feedstock concentration) on the product gas composition during hydrothermal gasification of biomass model compounds. In addition, this study also considered the interrelated effects between cellulose, hemicellulose and lignin as well as the above-mentioned process parameters on the overall gas yields during SCWG. To study the effects of experimental conditions and the interactions between the biomass model compounds, the response surface methodology (RSM) based on the Box-Behnken design (BBD) was implemented.

The traditional "one variable at a time" (univariate) approach is often used by many researchers to optimize a process and study the effects of various factors on the response. The method involves testing the effect of a single variable on a response by keeping other variables constant [33]. Although promising results have been achieved using this approach, the information about the actual interactions

Please cite this article as: Okolie JA et al., Optimization and modeling of process parameters during hydrothermal gasification of biomass model compounds to generate hydrogen-rich gas products, International Journal of Hydrogen Energy, https://doi.org/10.1016/j.ijhydene.2019.05.132

among the variables is less exposed. However, the RSM incorporates a set of statistical techniques that are used for modeling and model exploitation [37]. Through a meticulous design of experiments, the RSM attempts to establish the relationship that exists between a set of measured dependent variables (responses) and the controlled independent variables (experimental factors). This approach allows the development of mathematical models to predict the responses and study the statistical significance of the factors being studied [38]. Moreover, the interaction effects between the factors can be evaluated with minimal experimental runs, which is an added advantage.

To the best of our knowledge, this is the first study to implement BBD design for optimizing and studying the effects of process parameters including temperature, reaction time and feedstock concentration (biomass-to-water ratio) for maximum H_2 yield during SCWG of synthetic biomass comprising of cellulose, xylose and lignin. Initially, H_2 yields from hydrothermal gasification of cellulose was optimized following which the optimal reaction conditions were used to study the decomposition patterns and gaseous product distribution for other model compounds such as xylose and lignin. Cellulose was used for process optimization because in most of the available lignocellulosic biomasses, cellulose exhibits the largest composition compared to hemicellulose and lignin. Overall, lignocellulosic biomass consists of 30–60 wt% cellulose, 20–40 wt% hemicellulose and 15–25 wt % lignin on dry basis [11]. Finally, considering all the experimental results, a generic reaction pathway for synthetic biomass gasification in SCW was proposed. This study could provide a comprehensive knowledge useful for the identification of suitable biomass species and process conditions optimal for H_2-rich syngas production through hydrothermal gasification.

Materials and methods

Feedstock

Three different biomass model compounds (i.e. cellulose, hemicellulose, and lignin) were used to represent the synthetic lignocellulosic biomass. The model compounds such as cellulose, xylose (hemicellulose) and Kraft lignin were purchased from Sigma-Aldrich (Oakville, Canada). All model compounds were in high purity and in form of dry powder. Nitrogen, used as the inert gas, was purchased from Praxair Canada Inc. (Saskatoon, Canada).

Hydrothermal gasification experimental setup

Hydrothermal gasification experiments were performed in a tubular fixed-bed batch reactor made of stainless steel SS316 (length: 40 cm, outer diameter: 13 mm and inner diameter: 9 mm). Fig. 1 shows a schematic representation of the gasification setup. The gasification assembly consisted of SS316 materials purchased from Swagelok (Swagelok Central Ontario, Mississauga, Canada). The setup comprised of a tubular reactor enclosed inside an ATS Series 3210 furnace (Applied Test Systems, Butler, USA), thermocouples, pressure gauges, pressure relief valves, check valves, 2-μm filters, a gas-liquid separator, a desiccator and a temperature controller system.

For hydrothermal gasification experiment, synthetic biomass was loaded into the reactor together with the desired amount of water depending on the feedstock concentration. Prior to gasification experiment, a leak detection test was carried out to ensure safety relating to high-pressure and high-temperature operations. After the reactor assembly was ensured to be properly sealed, any trace amount of air was removed from the reactor by using a vacuum pump. Nitrogen gas was then used to purge the reactor, create an inert atmosphere and supply the initial pressure required for the experiments i.e. 5–10 MPa. In the next step, the split furnace was used to heat the reactor to the desired temperature. The Omega Type-K thermocouples (Spectris Canada Inc., Laval, Canada) were used to continuously monitor and record the reactor temperature. Once the gasification reaction was completed, the furnace was switched off and the reactor was cooled by spraying cold water. The gas products, volatiles and vapors entered the gas-liquid separating cylinder where the gases were collected using Tedlar bags and the liquid products were collected after condensation. The desiccator trapped the moisture from the gas products before injecting into a gas chromatography system. Finally, the solid biochar product was recovered after cooling the reactor.

Feedstock and product characterization

The ultimate analysis of the model biomass compounds (cellulose, xylose and lignin) was done to estimate the proportions of carbon, hydrogen, nitrogen, sulfur and oxygen using an Elementar Vario EL III CHNS analyzer (Elementar Analysensysteme, Hanau, Germany). The product gas composition from hydrothermal gasification of biomass model compounds was analyzed by an Agilent GC 7820A gas chromatograph (Agilent Technologies, Santa Clara, USA). The GC was equipped with a thermal conductivity detector (TCD) together with one capillary column and three packed columns. Ultimetal HayesepQ T 80/100 mesh column was used to measure the concentrations of H_2, CH_4 and CO while Ultimetal Hayesep T 80/100 mesh column was used to estimate the concentrations of CO_2 and C_2–C_4 gases. Argon was used as the carrier gas. The column and detector temperatures maintained at 60 °C and 50 °C, respectively.

The gas yield of each product gas component was expressed as the moles of each gas per gram of biomass feedstock used in the experiment (mmol/g) [15,39–41]. The total gas yield was expressed as the sum of individual gas yield expressed in mmol/g. The hydrogen selectivity was elucidated via Eq. (1) [18,23,24]. The lower heating value (LHV) was calculated using Eq. (2) [42], where H_2, CO, CH_4 and C_nH_m represent the molar concentrations of the product gases.

Hydrogen selectivity (HS):

$$HS\,(\%) = \left(\frac{\text{Moles of } H_2}{\text{Sum of moles of } CO, CO_2, CH_4 \text{ and } C_1 - C_4}\right) \times 100 \quad (1)$$

Lower heating value (LHV):

Please cite this article as: Okolie JA et al., Optimization and modeling of process parameters during hydrothermal gasification of biomass model compounds to generate hydrogen-rich gas products, International Journal of Hydrogen Energy, https://doi.org/10.1016/j.ijhydene.2019.05.132

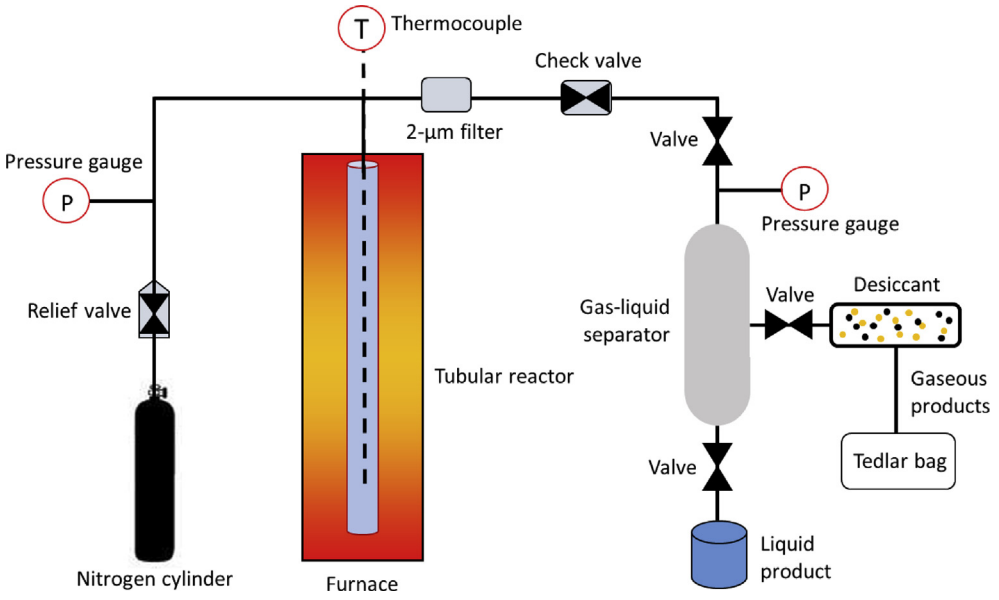

Fig. 1 – Schematics of the tubular hydrothermal gasification reactor.

$$\text{LHV}\ (\text{kJ}/\text{Nm}^3) = (30.3 \times \text{CO} + 25.8 \times \text{H}_2 + 85.4 \times \text{CH}_4 + 151.3 \times \text{C}_n\text{H}_m) \times 4.2 \quad (2)$$

Design of experiments for modeling and optimization studies

In this work, the RSM approach using a 3-level and 3-factor Box-Behnken design was used to optimize H_2 yields and study the influence of different process variables on the gas yield during the SCWG of cellulose. The independent process variables selected for the experimental studies are temperature (300–500 °C), reaction time (30–60 min) and feedstock concentration (10–30 wt%). H_2 yield expressed in mmol/g of feedstock was the dependent variable. Table 1 shows the investigated factors and levels for the Box-Behnken design. The center values selected for the experimental design were temperature (400 °C), reaction time (45 min) and feedstock concentration (20 wt%). The number of experiments required for the Box-Behnken design was calculated using Eq. (3), where k is the number of factors and C_0 is the number of center points.

$$N = 2k^2 - 2k + C_0 \quad (3)$$

Table 1 – Box- Behnken experimental design factors and factor levels used for hydrothermal gasification of cellulose.

Factor	Low level (−1)	Medium Level (0)	High Level (+1)
Temperature, T (°C)	300	400	500
Reaction time, R_t (min)	30	45	60
Feedstock concentration, C (wt%)	10	20	30

For this study, fifteen experimental runs containing triplicates at the center points were used. The experimental error was obtained using the center points. Design-Expert® Software version 8.0.7.1 (Stat Ease, Inc., Minneapolis, USA) was used to perform the experimental design and the runs were designed in a random order. The Box-Behnken design procedure includes carrying out the statistically planned experiments and a regression equation resulting from the fitting of the data to different models. The best model was selected based on the sequential sum of squares (*p*-value and *F*-value) and the model summary statistics (R^2 i.e. coefficient of determination), adjusted R^2, predicted R^2 and standard deviation). The equation was used to approximate relationships between the factors and their responses as well as for predicting the responses. The Box-Behnken design is advantageous because it requires that all factors be run at only three levels and they are rotational or almost rotational [43]. Moreover, there is a reduction in the number of experimental runs required for the design when compared to the 3-factors and 3-levels complete factorial design or the central composite design as reported by Kang et al. [33].

Results and discussion

Feedstock characterization

The ultimate analysis of cellulose, xylose and lignin used as the model compounds of the synthetic feedstock is shown in Table 2. Lignin had highest levels of carbon (47.4 wt%) followed by cellulose (42.5 wt%) and xylose (39.9 wt%). Cellulose did not show the presence of nitrogen and sulfur. On the contrary, lignin contained 0.1 wt% nitrogen and 3.9 wt% sulfur, while xylose had 0.1 wt% sulfur. Although the present study does not involve the use of catalyst, it should be noted that for catalytic reactions the presence of sulfur in lignin could deactivate the

Please cite this article as: Okolie JA et al., Optimization and modeling of process parameters during hydrothermal gasification of biomass model compounds to generate hydrogen-rich gas products, International Journal of Hydrogen Energy, https://doi.org/10.1016/j.ijhydene.2019.05.132

Table 2 – Ultimate analysis of cellulose, xylose and lignin.

Feedstock	Carbon (wt%)	Hydrogen (wt%)	Nitrogen (wt%)	Sulfur (wt%)	Oxygen (wt%)
Cellulose	42.5 ± 0.33	5.7 ± 0.83	0	0	51.8
Xylose	39.9 ± 0.07	5.9 ± 1.01	0	0.1 ± 0.11	54.1
Lignin	47.4 ± 0.12	4.8 ± 0.71	0.1	3.9 ± 0.07	43.8

Note: Oxygen composition (wt%) was calculated by the difference of C, H, N and S.

catalyst. Lignin also showed the lowest oxygen content (43.8 wt %) because of its lower degree of oxidation compared to cellulose and xylose. Xylose had the lowest carbon content (39.9 wt%) and the highest oxygen content (54.2 wt%). Lignin is a phenylpropane polymer consisting of highly branched and cross-linked C–H groups as opposed to cellulose (containing long chain glucose monomers) and hemicellulose (containing short chain pentose and hexose sugars) [11].

Hydrothermal gasification of synthetic biomass

The reaction conditions, H_2 yield and total mass balance for the products obtained from hydrothermal gasification of cellulose in subcritical and supercritical conditions are reported in Table 3. The total mass balance ranged from 84.9 wt% to 95.6 wt%. The loss in mass could be due to the difficulties encountered during product collection leading to certain product losses. For instance, some char particles (mostly char fines) trapped in the gas-liquid separator entrained in the liquid effluents. Such challenges in the mass balance during hydrothermal gasification of biomass has also been reported in literature [33,41,44]. For example, Ding et al. [41] reported a mass balance of 53–59.8 wt% during SCWG of cellulose. Similarly, Kang et al. [33] obtained a mass balance between 85.9 wt% and 93.5 wt% during SCWG of lignin.

As seen in Table 3 (ca. experimental run 3), the maximum H_2 yield of 1.94 mmol/g was obtained from cellulose gasification under supercritical conditions (500 °C, 20 wt% feedstock concentration and 60 min). In contrast, lowest yield of H_2 was obtained from cellulose gasification under subcritical conditions (300 °C, 30 wt% feedstock concentration and 45 min) (Table 3, experimental run 7). The H_2 yield increased with temperature from 300 °C (subcritical water gasification) to 500 °C (supercritical water gasification) due to enhanced water-gas shift reaction and steam reforming reaction [45,46]. Water-gas shift reaction is a reaction between water vapor and CO to produce CO_2 and H_2. The reaction is favored at high temperatures (Eq. (4)).

Water-gas shift reaction:

$$CO + H_2O \leftrightarrow CO_2 + H_2 \ (\Delta H = -41 \text{ kJ/mol}) \quad (4)$$

Steam reforming reaction:

$$C_6H_{12}O_6 + 6H_2O \rightarrow 6CO_2 + 12H_2 (\Delta H = +206 \text{ kJ/mol}) \quad (5)$$

Lee et al. gasified glucose as a model compound of cellulose in SCW at a temperature range of 470–750 °C under a constant pressure of 28 MPa [31]. The authors observed a rapid increase in H_2 yields with temperature above 660 °C with a subsequent decrease in CO yield. The carbon gasification efficiency also approached 100% at about 700 °C. Therefore, greater SCW

Table 3 – Experimental conditions, experimental and predicted hydrogen yields and mass balance from hydrothermal gasification of cellulose.

Experiment number	Temperature, T (°C)		Reaction time, R_t (min)		Feedstock concentration, C (wt %)		Hydrogen yield (mmol/g)		Overall mass balance (wt%)
	T (Coded)	T (Uncoded)	R_t (Coded)	R_t (Uncoded)	C (Coded)	C (Uncoded)	Experimental Value	Predicted Value	
1	0	400	1	60	−1	10	1.18	1.21	88.7
2	0	400	0	45	0	20	0.88	0.91	95.2
3	1	500	1	60	0	20	1.94	1.89	91.6
4	−1	300	−1	30	0	20	0.64	0.69	93.9
5	1	500	−1	30	0	20	1.36	1.35	92.4
6	−1	300	0	45	−1	10	0.69	0.65	94.9
7	−1	300	0	45	1	30	0.56	0.53	87.4
8	0	400	−1	30	1	30	0.90	0.88	87.7
9	0	400	0	45	0	20	0.99	0.91	94.8
10	0	400	0	45	0	20	0.85	0.91	89.9
11	1	500	0	45	−1	10	1.44	1.47	94.8
12	1	500	0	45	1	30	1.49	1.53	84.9
13	−1	300	1	60	0	20	0.72	0.73	91.7
14	0	400	−1	30	−1	10	0.72	0.70	94.4
15	0	400	1	60	1	30	0.94	0.91	95.6

Note: The data presented for experimental hydrogen yield (mmol/g) are from experiments carried out in triplicates with standard error < 5%.

Please cite this article as: Okolie JA et al., Optimization and modeling of process parameters during hydrothermal gasification of biomass model compounds to generate hydrogen-rich gas products, International Journal of Hydrogen Energy, https://doi.org/10.1016/j.ijhydene.2019.05.132

temperature of 500 °C was found to be optimal for maximum H_2 yields in this study.

Statistical evaluation and determination of regression model

As mentioned earlier, 15 experimental runs were carried out in triplicates in this study and regression analysis was used to estimate the coefficients of the model. To obtain the optimum conditions for H_2 yield and investigate the effect of process conditions, the experimental runs were performed in accordance with the experimental design in Table 1. The regression equation for understanding the relationship between H_2 yield and temperature, reaction time and feedstock concentration was obtained by fitting of the data to different models such as linear, quadratic, interactive and cubic. The adequacy of the models was determined by the sequential model sum of squares and the model summary statistics [47], after which a multiple regression was performed to estimate the coefficients present in the mathematical model. The obtained model, which was used to predict H_2 yield was compared with the experimental yield as shown in Table 3.

The results of the model adequacy verification are presented in Table S1 and Table S2 (supplementary materials). From the sequential model sum of squares table, it should be noted that a model with a low *p*-value (probability value) and high *F*-value are said to be significant. In addition, a model with non-significant lack of fit (*p*-value > 0.05) is also desirable. The *F*-value provides an indication of how each controlled factor affects the tested model. It can be defined as the ratio of regression mean square and mean of the real error [47]. On the other hand, the associated *p*-value evaluates whether the *F*-value is large enough to demonstrate statistical significance. The non-significant lack of fit confirms that the model fits properly with the response and the data can be used to interpret the model adequately [48]. From the lack of fit test, the quadratic model was observed to be highly insignificant with *p*-value of 0.5912 and was suggested as the best model.

The model summary statistics was also used to verify the model adequacy based on the values of R^2 (coefficient of determination), adjusted R^2, predicted R^2 and standard deviation (Table S2). The quadratic model had the maximum adjusted R^2 (0.968), predicted R^2 (0.8878) (Table S2). The adjusted R^2 is the value of R^2 that has been adjusted to account for different number of predictors in a model. Furthermore, the quadratic model exhibited the lowest standard deviation of 0.07. The standard deviation, which is a measure of variability indicates the deviation of the model data from the mean. The lower the standard deviation, more closely the data points are arranged to the mean. It should be noted that although the cubic model had the highest R^2 value (0.9949) compared to the quadratic model (0.968), the quadratic model was suggested based on the adjusted R^2 value and standard deviation. Based on the results from the sequential sum of squares and model summary statistics, the quadratic model was selected to represent the relationship between H_2 yield and process conditions (i.e. temperature, reaction time and feedstock concentration). By using multiple regression analysis, the second-order equation obtained including the linear, square and interaction terms in coded factors is represented in Eq. (6):

$$Y_i = 0.91 + 0.45T - 0.81C + 0.15R + 0.048TC + 0.13TR - 0.1CR_t + 0.18T^2 - 0.048C^2 + 0.074R_t^2 \quad (6)$$

where, Y_i denotes H_2 yield in mmol/g; T, C and R_t denotes the hydrothermal gasification temperature (°C), feedstock concentration (wt%) and reaction time (min), respectively. In addition, TC, TR_t and CR_t represent the process interactions such as temperature-feedstock concentration, temperature-reaction time and feedstock concentration-reaction time, respectively. On the other hand, T^2, C^2 and R_t^2 signify the square term of the model. The predicted response for H_2 yield using the quadratic model correlates well with the experimental results as shown in Table 3.

The analysis of variance (ANOVA) was used to ascertain whether each independent variable and its interactions were significant. The value of alpha (α), used to evaluate the statistical significance in this study, is 0.05. A p-value $\leq$ 0.05 means that the model and all the terms associated with it are statistically significant [49]. Similarly, a large *F*-value means that the equation can explain the variation in the response adequately. Other descriptive statistics used to further assess the goodness of fit for the model include R^2, adjusted R^2, predicted R^2, sum of squares, coefficient of variation and the mean sum of squares. The ANOVA results presented in Table S3 (supplementary materials) show that the model has an *F*-value of 48.1 and *p*-value of 0.0003, which imply that the model is highly significant. For each individual term of the model, a *p*-value < 0.05 means that they are significant. The most significant parameter that affects H_2 yield is temperature with a *p*-value < 0.0001. The reaction time was also significant with *p*-value of 0.0019.

The interaction effects, especially TR_t (temperature-reaction time) and CR_t (feedstock concentration-reaction time) together with the square term for temperature (T^2) and reaction time (R_t^2) were also found to be significant. In general, two interaction terms and two square terms were found to be significant. The *F*-value of 0.82 and *p*-value of 0.5912 imply that the lack of fit is insignificant with respect to the pure error. Non-significant lack of fit is preferable for the model fit. To determine how well the model fits, R^2 and adjusted R^2 values were assessed. The value of R^2 (0.9886) implies that 98.9% of the variation in the response can be explained by the model (Table S3). On the other hand, the adjusted R^2 value of 0.9680 further confirms the significance of the model [50]. The adjusted R^2 is the modified value of R^2 that has been adjusted to compare models with different number predictors since R^2 value increases whenever a predictor is added to a model. Therefore, the adjusted R^2 is suggested to be a better criterion. For new observations, the predicted R^2 helps to evaluate how well the model can predict the response. The predicted R^2 value of 0.8878 is in good agreement with the adjusted R^2 value. The results in Table S3 confirms that the equation is an actual representation of the relationship between the experimental conditions (factors) and H_2 yields (response).

To show the correlation between the experimental and predicted values, a parity plot is presented in Fig. 2. The parity

Please cite this article as: Okolie JA et al., Optimization and modeling of process parameters during hydrothermal gasification of biomass model compounds to generate hydrogen-rich gas products, International Journal of Hydrogen Energy, https://doi.org/10.1016/j.ijhydene.2019.05.132

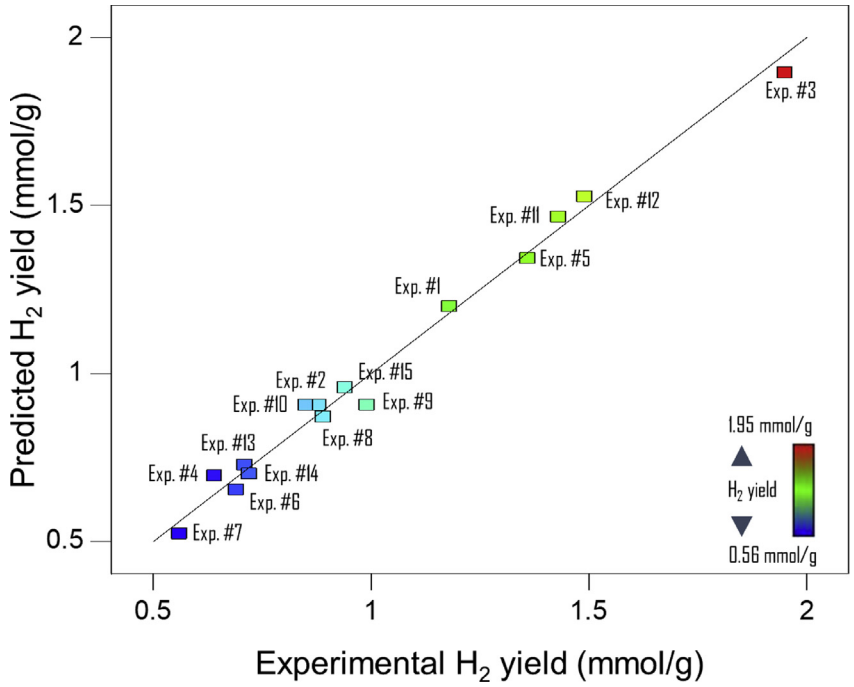

Fig. 2 – Parity plot showing the comparison between the experimental and predicted H_2 yield from different experimental runs during hydrothermal gasification of cellulose at 300–500 °C with 10–30 wt% feed concentration in 30–60 min.

plot exhibits a satisfactory correlation between the observed and predicted values of H_2 yield. The data points are found to cluster around the straight line, which implies that there is a good agreement between the observed and predicted values. The normality of the dataset was also verified using the normal probability plot of the residuals as shown in Fig. 3. The residuals indicate the variation between the observed value of the response (H_2 yield) and the value obtained under the theoretical model. The normality plot is a useful diagnostic tool that is used to identify and explain the deviations from the assumptions that the errors are normally distributed, their variances are consistent, and they are independent of each

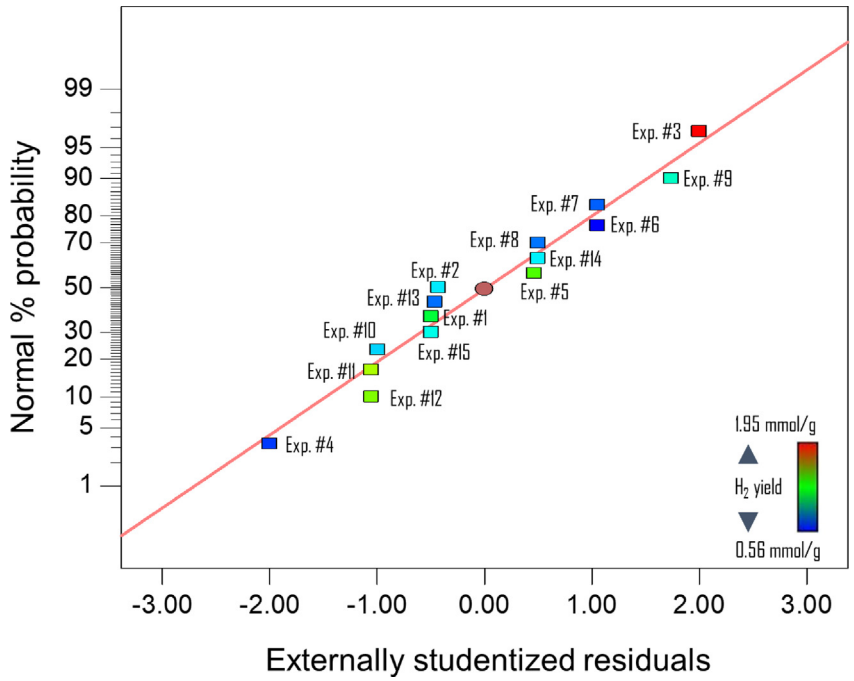

Fig. 3 – Normal probability plots of the residuals for H_2 yield from different experimental runs during hydrothermal gasification of cellulose at 300–500 °C with 10–30 wt% feed concentration in 30–60 min.

Please cite this article as: Okolie JA et al., Optimization and modeling of process parameters during hydrothermal gasification of biomass model compounds to generate hydrogen-rich gas products, International Journal of Hydrogen Energy, https://doi.org/10.1016/j.ijhydene.2019.05.132

other [43]. As seen in Fig. 3, the data points are reasonably close to the straight line, which shows that the data are normally distributed.

Effects of experimental factors and their interactions on hydrogen yield

Hydrothermal gasification of cellulose was performed at pressure ranges of 23–25 MPa to study the impacts of temperature (300–500 °C), reaction time (30–60 min) and feedstock concentration (10–30 wt%). The 3D response surface plots and 2D contour plots are useful in understanding the influence of experimental factors and their interactions on the responses and obtain the optimal values of the variables within the study range. The plots are usually expressed as a function of two factors while the other factors are kept constant. Therefore, the 3D response surface plots and 2D contour plots were used in this study to investigate the influence of temperature, feedstock concentration and reaction time on H_2 yield. Since there are only three factors used for the regression model, one of the variables was kept constant at the center point for each of the plots. The 3D response surface plots as a function of two experimental variables (reaction time and temperature) with one variable fixed (feedstock concentration) at the center point and 2D contour plots are presented in Fig. 4. In Fig. 5, the reaction time was kept constant while the feedstock concentration and temperature were varied.

It is evident from Figs. 4 and 5 that H_2 yield increases with temperature and reaction time. As the temperature increases from 300 °C (subcritical conditions) to 500 °C (supercritical condition), two reaction pathways are inherent, i.e. the ionic pathway and free radical pathway [8]. The ionic pathway is dominant at subcritical conditions, whereas the free radical pathway is favorable at supercritical conditions. As the temperature elevates from 300 °C to 500 °C, the ionic product concentration i.e. K_w (H^+ and OH^-) also increases up to a maximum value at around 300 °C before decreasing at higher temperatures [19]. The initial increase in ionic concentration provides more hydronium ions (H_3O^+), thereby facilitating acid-catalyzed reactions. Besides, the decrease in K_w at higher temperatures from subcritical to supercritical water gasification is attributed to a decrease in the density of water. This also leads to enhanced free radical mechanisms as low water density is preferable for free radical reactions [35,45]. The free radical mechanisms play a major role in improved solvation of organic compounds, thereby leading to enhanced gas yields. Like temperature, an increase in reaction time from 30 to 60 min led to a subsequent rise in H_2 yields. In the present study, an increase in H_2 yield with temperature and reaction time was observed during the SCWG of cellulose. Keeping the other parameters constant, H_2 yield elevated from 0.56 mmol/g at 300 °C (experimental run 7) to 1.94 mmol/g at 500 °C (experimental run 3) (Table 3). In the same way, as the reaction time prolonged from 30 min to 60 min, the H_2 yield increased from 0.64 mmol/g (experimental run 4) to 1.94 mmol/g (experimental run 3).

Longer reaction time leads to improved H_2 yields by enhancing the primary reactions taking place under supercritical conditions [18]. The primary reactions occurring under high temperature in supercritical conditions include bond cleavage, dehydration, decarboxylation, deamination and depolymerization [51]. Regarding the interactions between reaction time and temperature, it should be mentioned that the effect of increasing reaction time on H_2 yield at supercritical conditions was more pronounced than at subcritical conditions. For instance, at 300–400 °C, the interactions between reaction time and temperature was weaker. The H_2 yield remained at about 0.8 mmol/g with an increase in reaction time from 30 min to 60 min at the temperature range of 300–400 °C (Fig. 4b). This shows that an increase in reaction time from 30 min to 60 min had an insignificant increase in H_2 yield. When the temperature increased up to 500 °C, the interaction between H_2 yield and temperature became significant as the H_2 yield starts to increase with longer reaction time. This behavior could be a result of the formation of char and tar from partially decomposed biomass at low temperatures in subcritical conditions [52,53].

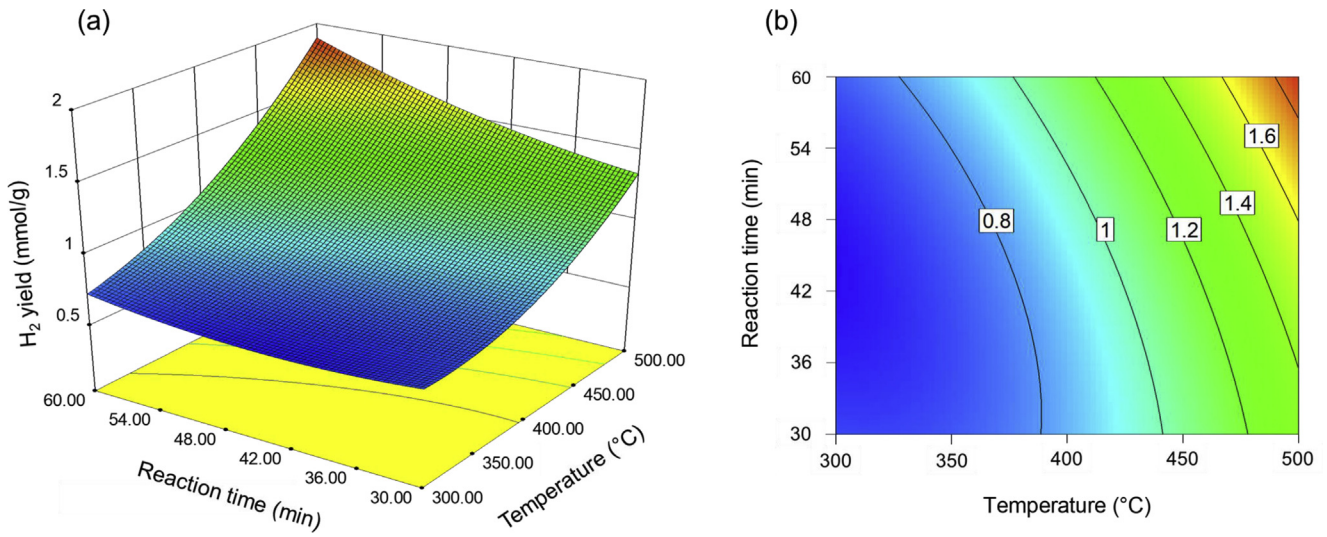

Fig. 4 – (a) 3D response surface plot and (b) 2D contour plot showing the influence of reaction time and temperature on H_2 yield from hydrothermal gasification of cellulose.

Please cite this article as: Okolie JA et al., Optimization and modeling of process parameters during hydrothermal gasification of biomass model compounds to generate hydrogen-rich gas products, International Journal of Hydrogen Energy, https://doi.org/10.1016/j.ijhydene.2019.05.132

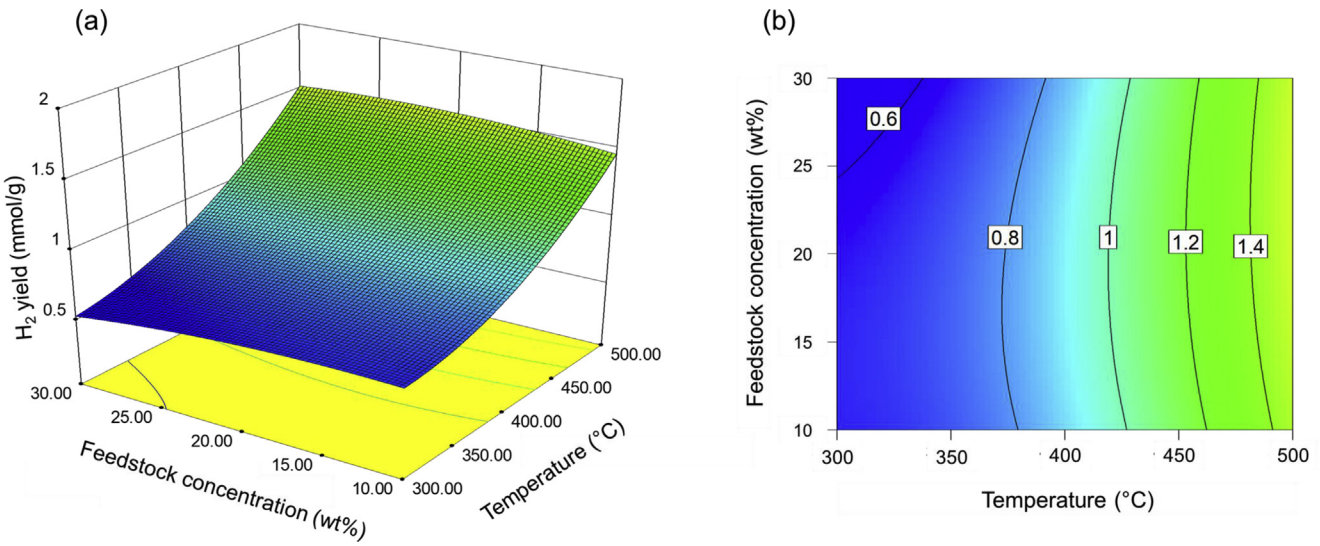

Fig. 5 – (a) 3D response surface plot and (b) 2D contour plot showing the influence of feedstock concentration and temperature on H_2 yield from hydrothermal gasification of cellulose.

Char and tar are polymeric compounds that are highly challenging to breakdown even at longer reaction time restricting further degradation of the feedstock intermediates and gas formation [53–55]. Similar results was obtained by Tiong et al. [56] during the SCWG of microalgae *Chlorella vulgaris* and *Scenedesmus quadricauda*. The amount of gas yield remains almost the same by increasing the reaction time more than 30 min at 385 °C and 26 MPa. A recent study by Samiee-Zafarghandi et al. [57] also reported a similar trend. They investigated the gasification of microalgae in SCW at a temperature range of 355–405 °C, reaction time of 15–45 min and biomass loading of 1–8 wt%. By increasing the reaction time from 15 min to 45 min at 405 °C (supercritical conditions), the H_2 yield improved from 13.3 mol% to 20.9 mol%. However, at 355 °C (subcritical conditions), the increase in H_2 yield was insignificant (1.1–1.2 mol%).

Concerning the influence of the feedstock concentration on H_2 yield, a negative effect occurs on H_2 yield at higher feedstock concentration. A negative coefficient of feedstock concentration (represented as C in Eq. (5)) in the regression model presented in Eq. (5) also confirms the negative effect. Furthermore, the interaction between feedstock concentration and temperature is insignificant (Table S3). Therefore, an increase in the feedstock concentration means a decrease in water molecules compared to the amount of feedstock. Similarly, a reduction in feedstock concentration translate into higher amount of water molecules compared to the feedstock. The high amount of water molecules leads to enhanced solvation properties in SCW, better solvation of biomass and improved gas yields. Since a majority of the H_2 produced from SCWG is supplied by water acting as a reactant [58], it is imperative to have excess amount of water to achieve high H_2 yield from biomass. The excess amount of water can be provided at low feedstock concentration.

Optimization of hydrogen yield

In the present study, the Box-Behnken design with 3-factors and 3-levels were employed to obtain the best combination of experimental conditions (i.e. temperature, feedstock concentration and reaction time) to produce the maximum H_2 yield. The numerical optimization function in Design-Expert® software was used for the process optimization. All the variables are set within the experimental limits, i.e. temperature ranges: 300–500 °C, feedstock concentration: 10–30 wt% and reaction time ranges of 30–60 min (Fig. 6). According to the 3D surface plot in Fig. 4, at 500 °C, 60 min and 20 wt% feedstock concentration, the highest H_2 yield obtained was 1.89 mmol/g. Therefore, the value of H_2 yield in the optimizer was set to be greater than or equal to 1.9 mmol/g in the Design-Expert® software. The numerical optimization produced a maximum H_2 yield of 1.92 mmol/g at optimal reaction conditions of 500 °C, 60 min and 12.5 wt% feedstock concentration. By using the obtained reaction conditions, a test experimental run was carried out to validate the model. The value of H_2 yield obtained from the experimental run at optimal conditions (temperature: 500 °C, reaction time: 60 min and feedstock concentration: 12.5 wt%) was 1.95 mmol/g. The percentage error between the experimental and predicted values was calculated using Eq. (7). The percentage error between the experimental and predicted result was found to be less than 2%.

$$\text{Percent Error} = \frac{(\text{Experimental value of } H_2 \text{ yield} - \text{Predicted value of } H_2 \text{ yield})}{\text{Experimental value of } H_2 \text{ yield}} \times 100 \quad (7)$$

Please cite this article as: Okolie JA et al., Optimization and modeling of process parameters during hydrothermal gasification of biomass model compounds to generate hydrogen-rich gas products, International Journal of Hydrogen Energy, https://doi.org/10.1016/j.ijhydene.2019.05.132

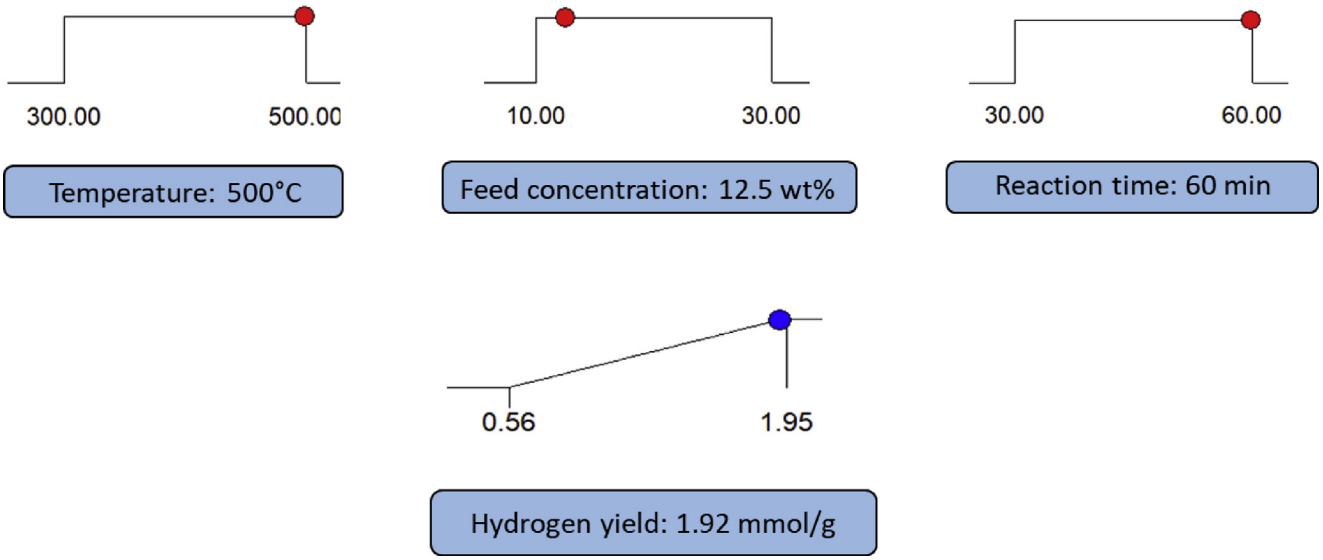

Fig. 6 – Experimental limits set for each process conditions and the response (H_2 yield) together with their optimal values.

SCWG of biomass model compounds

The model compounds representing cellulose, xylose and lignin were gasified at optimal conditions (temperature: 500 °C, feedstock concentration: 12.5 wt% and reaction time: 60 min) to compare their gas yield and understand the behavior of each component under supercritical conditions. The distribution of the gaseous products was useful for the prediction of reaction mechanism of model compounds and their decomposition patterns. Fig. 7 shows the gaseous product distribution of the SCWG of biomass model compounds at optimal reaction conditions. As seen in Fig. 7, gases produced during the gasification of lignocellulosic model compounds are CO_2, H_2, CH_4, CO and C_2–C_4 hydrocarbons. Almost half of the H_2 is supplied by the water reactant through the water-gas shift reactions while CH_4 production is attributed to methanation and hydrogenation reactions [59,60]. The methanation reaction is a reaction that consumes H_2 to produce CH_4 and water as shown in Eqs. (8) and (9). However, it should be noted that since H_2 is the desired product of SCWG, methanation reaction should be suppressed while enhancing the water-gas shift reaction, which is achieved through the application of selective catalysts.

Methanation reaction of CO:

$$CO + 3H_2 \rightarrow CH_4 + H_2O \ (\Delta H = -206.2 \text{ kJ/mol}) \quad (8)$$

Methanation reaction of CO_2:

$$CO_2 + 4H_2 \rightarrow CH_4 + 2H_2O \ (\Delta H = -206.2 \text{ kJ/mol}) \quad (9)$$

Hydrogenation reaction of CO:

$$CO + 2H_2 \rightarrow CH_4 + 0.5O_2 \ (\Delta H = -131 \text{ kJ/mol}) \quad (10)$$

Hydrogenation reaction of CO_2:

$$CO_2 + 2H_2 \rightarrow C + 2H_2O \ (\Delta H = -90 \text{ kJ/mol}) \quad (11)$$

The product gas distribution varies for all the model compounds, which indicates that properties such as functional groups and chemical linkages influence biomass decomposition and gas evolution under SCW conditions [54]. Cellulose demonstrated highest CO_2 (3.24 mmol/g), CO (0.17 mmol/g) and CH_4 (1.79 mmol/g) yields (Fig. 7). Furthermore from Fig. 7, H_2 yield decreases in the order of xylose (2.26 mmol/g) > cellulose (1.95 mmol/g) > lignin (0.73 mmol/g). Similar trend was obtained by Sivasangar et al. [54]. They stated that the highest H_2 yield was obtained from the model compound representing hemicellulose. This could be because of the decomposition of formic acid produced during the hydrolysis of xylose to form CO_2 and H_2 under SCW conditions. Highest H_2 selectivity was also found in the case of xylose (57.9%) as shown in Table 4. Cellulose demonstrated highest CO_2 (3.24 mmol/g), CO (0.17 mmol/g) and CH_4 (1.79 mmol/g) yields (Fig. 7).

The molecular weights of cellulose, hemicellulose (xylose) and lignin are 342 g/mol, 150 g/mol and 1514 g/mol [61]. Moreover, the degree of polymerization of cellulose is 1510–5500, whereas for hemicellulose it is 50–200 [62]. Each cellulose polymer comprises of long-chain polysaccharide with 7000–15,000 glucose monomers, whereas each short-chain polysaccharide in hemicellulose consists of 500–3000 glucose monomers. In addition, cellulose is mostly present in both crystalline and amorphous forms while hemicellulose is amorphous and easily hydrolysable. Owing to the relatively lower degree of polymerization and lower molecular weight and short-chain nature, hemicellulose (xylose) is easily hydrolyzed and gasified in hydrothermal gasification compared to cellulose and lignin, which require more intense reaction conditions for near-complete conversion.

The gases such as CO and CO_2 are produced because of the cleavage of functional groups such as carboxyl and carbonyl groups that are present in the basic subunits of lignocellulosic biomass [54]. However, CO is consumed during the water-gas shift reaction, which explains the lowest amount of CO compared to all gases produced in the model compounds. Another explanation for the high concentration of CO and CO_2 in cellulose compared to xylose and lignin could be because

Please cite this article as: Okolie JA et al., Optimization and modeling of process parameters during hydrothermal gasification of biomass model compounds to generate hydrogen-rich gas products, International Journal of Hydrogen Energy, https://doi.org/10.1016/j.ijhydene.2019.05.132

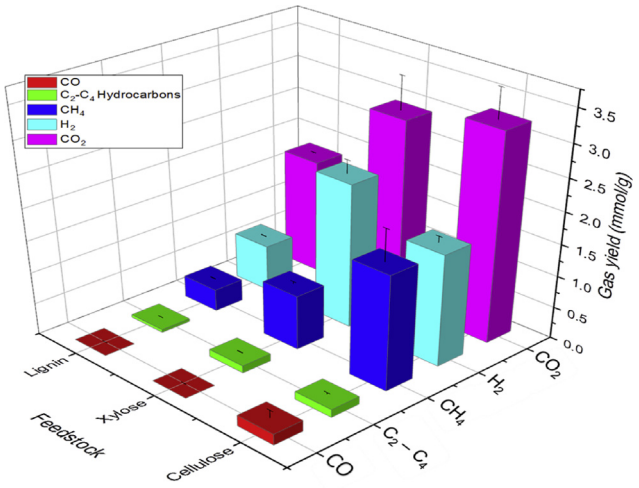

Fig. 7 – Gas yields from supercritical water gasification of cellulose, xylose and lignin at optimal process conditions (temperature: 500 °C, feedstock concentration: 12.5 wt% and reaction time: 60 min).

cellulose has a higher amount of carbonyl and carboxyl functional groups in its chemical structures [63]. Cellulose is a polymer of glucopyranose linked together by β-1,4 D-glucose subunits and rich in C–O and O–H groups compared to hemicellulose and lignin [54,64]. The hydrothermal cleavage of such functional groups presents in cellulose results in the production of high concentrations of CO and CO_2.

Among all the model compounds, the total gas yield decreased as xylose (6.16 mmol/g) > cellulose (5.97 mmol/g) > lignin (2.92 mmol/g) (Table 4). Furthermore, the gaseous products from cellulose exhibited the highest LHV of 935.7 kJ/Nm^3 followed by xylose (626.1 kJ/Nm^3) while the gaseous products from the SCWG of lignin had the lowest LHV of 231.7 kJ/Nm^3. The LHV is defined as the heat released during the combustion of a specific amount of biomass initially at room temperature and then cooling the products obtained from the combustion to 150 °C. This considers that the latent heat of vaporization of water in the reaction products is excluded [41]. An increase in the LHV of the gaseous products from cellulose compared to those from other model compounds was due to the superior concentrations of CO, CH_4 and C_2–C_4 hydrocarbons found in the gas products obtained from SCWG of cellulose.

Table 4 – Total gas yields, hydrogen selectivity and lower heating value of gas products obtained from SCWG of biomass model compounds at optimal conditions (temperature: 500 °C, feedstock concentration: 12.5 wt% and reaction time: 60 min).

Model compound	Total gas yield (mmol/g)	Hydrogen selectivity (%)	Lower heating value (kJ/Nm^3)
Cellulose	5.97	32.8	935.7
Xylose	6.16	57.9	626.1
Lignin	2.92	33.3	231.7

Proposed reaction pathway for hydrothermal gasification of lignocellulosic biomass

Based on our experimental observations, a possible pathway for the hydrothermal gasification of lignocellulosic biomass in subcritical and supercritical water was proposed (Fig. 8). Lignocellulosic biomass is a complex mixture that consists of three main functional groups, namely cellulose, hemicellulose and lignin. During SCWG, two reaction mechanisms are inherent such as the ionic mechanism, which occurs at low subcritical temperatures and the free radical mechanism, which occurs at higher supercritical temperature (>500 °C). At temperature and pressure above the critical point of water, there is a decrease in density, ionic product and dielectric constant of water, which leads to enhanced free radical mechanisms at the same time inhibiting ionic mechanism [19,65]. Under subcritical temperatures, lignocellulosic biomass initially undergoes hydrolysis reaction to produce hydrolyzed products.

Carbohydrates such as cellulose and hemicellulose degrade into monomeric pentose and hexose sugars (e.g. glucose, xylose, arabinose, mannose, rhamnose, etc.), whereas lignin decomposes into phenolic compounds and formaldehydes (e.g. guaiacol, cathecol, syringol and cresol) [66]. The hydrolysis products of cellulose and hemicellulose are further converted via intermediate degradation into furfurals and hydroxymethylfurfural. These intermediate products further dissociate into permanent gases (e.g. CO_2, CO, H_2, CH_4 and C_2–C_4 gases) via ionic mechanisms. The phenolic compounds generated during the hydrolysis of lignin have the tendency to react and polymerize into heavier molecular weight compounds such as tar and char at longer reaction times. On the contrary, when free radical mechanisms dominate, the carbohydrates and organic acids produced during the hydrolysis of cellulose undergo secondary hydrolysis to produce aldehydes, phenolics and aromatics to further degrade into product gases. The concentration of product gases is dependent on the reaction temperature, reaction time, feedstock concentration and the interactions between these parameters. These parameters influence gasification reactions e.g. water-gas shift reaction, methanation, hydrogenation and Boudouard reactions [8]. The mechanisms of water-gas shift, methanation and hydrogenation reactions have been discussed in the previous sections. Boudouard reaction results in char and coke formation with the consumption of CO as shown in Eq. (12).

Boudouard reaction:

$$2CO \leftrightarrow C + CO_2 \ (\Delta H = -172 \text{ kJ/mol}) \quad (12)$$

It should be noted that the above-mentioned reactions are important during the stoichiometric thermodynamic modeling of SCWG. The stoichiometric approach involves performing different calculations to obtain equilibrium among the identified reactions, which can theoretically predict the gaseous product distribution for any lignocellulosic biomass [29]. This approach has been implemented by several researchers to analyze reaction behavior and optimize process conditions during SCWG [67–69].

Please cite this article as: Okolie JA et al., Optimization and modeling of process parameters during hydrothermal gasification of biomass model compounds to generate hydrogen-rich gas products, International Journal of Hydrogen Energy, https://doi.org/10.1016/j.ijhydene.2019.05.132

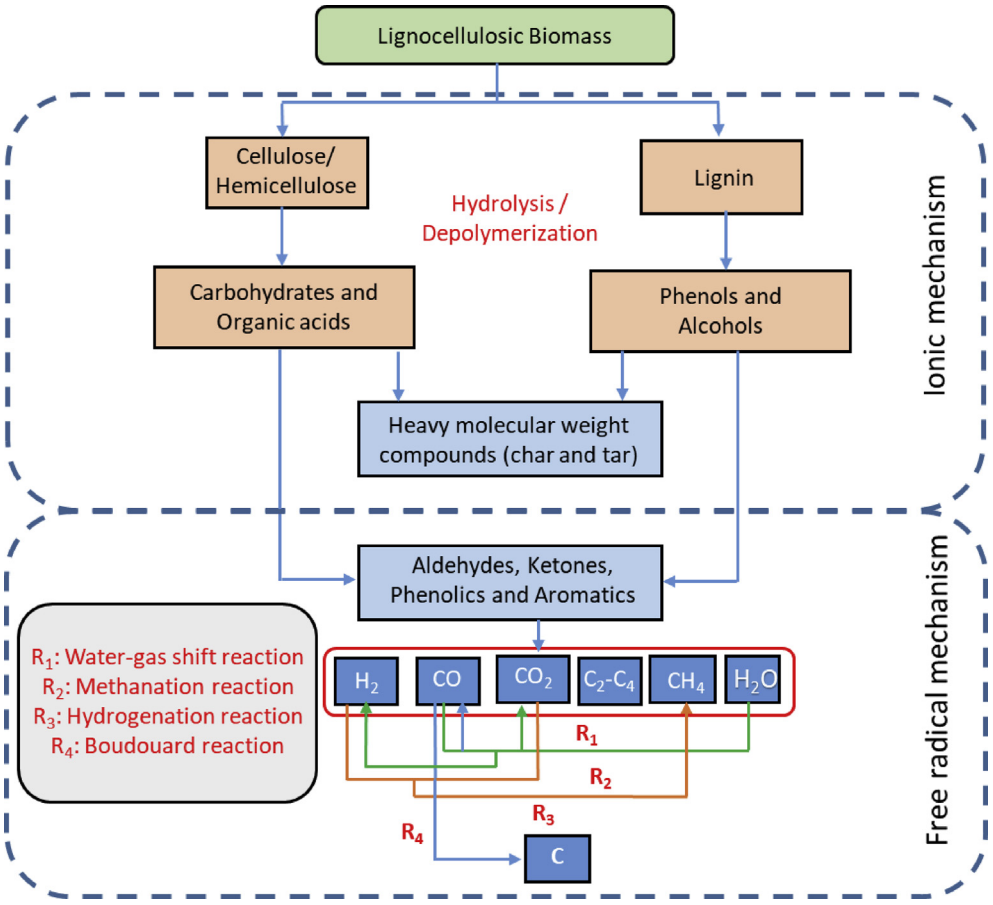

Fig. 8 – Reaction pathway during hydrothermal gasification of lignocellulosic biomass.

As mentioned earlier, during SCWG, water could act as an organic solvent by producing free radicals that take part in the decomposition of organic components. SCW also behaves as a catalyst and the reaction medium, thereby promoting the degradation of lignocellulosic biomass into mostly combustible gases. However, the high temperature requirements for SCWG is still a concern, due to the cost involved, challenges in selecting a suitable reactor material to withstand harsh conditions and the potential risks of char/tar-induced plugging issues. Therefore, various homogeneous and heterogeneous catalysts are used to improve gas yield and reduce char/tar formation while simultaneously decreasing temperature requirements.

Conclusions

The RSM method based on the Box-Behnken design was applied to study the hydrothermal gasification of cellulose as a lignocellulosic biomass model compound for the first time. The parameters studied were temperature (300–500 °C), reaction time (30–60 min) and feedstock concentration (10–30 wt%). Maximum H_2 yield of 1.95 mmol/g was obtained at 500 °C with 12.5 wt% feedstock concentration in 60 min of reaction time. A comparative evaluation of the SCWG of biomass model compounds representing cellulose, xylose and lignin shows that xylose had the highest H_2 yield of 2.26 mmol/g. Lignin had the lowest H_2 yield (0.73 mmol/g), which is attributed to its highly polymeric and recalcitrant chemical structure difficult to decompose even at supercritical conditions. The disparity in product gas composition between the model compounds signifies that chemical linkages and functional groups influence the decomposition patterns and the gaseous products formed during SCWG process. The reactant water through the water-gas shift reaction supplies majority of the H_2 in the syngas. The total gas yields for the model compounds decreased in the following order: xylose (6.16 mmol/g) > cellulose (5.97 mmol/g) > lignin (2.92 mmol/g). Based on the experimental observations, many important reactions involved in product gas formation during SCWG such as water-gas shift reaction, steam reforming reaction, methanation, hydrogenation and Boudouard reaction were identified. These reactions are useful during the stoichiometric thermodynamic analysis to predict gas yield and composition.

Acknowledgements

The authors would like to thank Natural Sciences and Engineering Research Council of Canada (NSERC) and Canada Research Chair (CRC) program for the financial support to conduct this energy research.

Please cite this article as: Okolie JA et al., Optimization and modeling of process parameters during hydrothermal gasification of biomass model compounds to generate hydrogen-rich gas products, International Journal of Hydrogen Energy, https://doi.org/10.1016/j.ijhydene.2019.05.132

Appendix A. Supplementary data

Supplementary data to this article can be found online at https://doi.org/10.1016/j.ijhydene.2019.05.132.

REFERENCES

[1] Nanda S, Azargohar R, Dalai AK, Kozinski JA. An assessment on the sustainability of lignocellulosic biomass for biorefining. Renew Sustain Energy Rev 2015;50:925–41.
[2] Nanda S, Rana R, Zheng Y, Kozinski JA, Dalai AK. Insights on pathways for hydrogen generation from ethanol. Sustain Energ Fuel 2017;1:1232–45.
[3] Okolie JA, Rana R, Nanda S, Dalai AK. Kozinski JA Supercritical water gasification of biomass: a state-of-the-art review of process parameters, reaction mechanisms and catalysis. Sustain Energ Fuel 2019;3:578–98.
[4] Levin DB, Chahine R. Challenges for renewable hydrogen production from biomass. Int J Hydrogen Energy 2010;35:4962–9.
[5] Bej B, Pradhan NC, Neogi S. Production of hydrogen by steam reforming of ethanol over alumina supported nano-NiO/SiO_2 catalyst. Catal Today 2014;237:80–8.
[6] Singh S, Kumar R, Setiabudi HD, Nanda S, Vo DVN. Advanced synthesis strategies of mesoporous SBA-15 supported catalysts for catalytic reforming applications: a state-of-the-art review. Appl Catal Gen 2018;559:57–74.
[7] Reddy SN, Nanda S, Kozinski JA. Supercritical water gasification of glycerol and methanol mixtures as model waste residues from biodiesel refinery. Chem Eng Res Des 2016;113:17–27.
[8] Correa CR, Kruse A. Supercritical water gasification of biomass for hydrogen production – Review. J Supercrit Fluids 2017;133:573–90.
[9] Nanda S, Mohanty P, Pant KK, Naik S, Kozinski JA, Dalai AK. Characterization of North American lignocellulosic biomass and biochars in terms of their candidacy for alternate renewable fuels. Bioenerg Res 2013;6:663–77.
[10] Azargohar R, Nanda S, Dalai AK, Kozinski JA. Physico-chemistry of biochars produced through steam gasification and hydro-thermal gasification of canola hull and canola meal pellets. Biomass Bioenergy 2019;120:458–70.
[11] Nanda S, Mohammad J, Reddy SN, Kozinski JA, Dalai AK. Pathways of lignocellulosic biomass conversion to renewable fuels. Biomass Conv Biorefin 2014;4:157–91.
[12] Holladay JD, Hu J, King DL, Wang Y. An overview of hydrogen production technologies. Catal Today 2009;139:244–60.
[13] Kalinci Y, Hepbasli A, Dincer I. Biomass-based hydrogen production: a review and analysis. Int J Hydrogen Energy 2009;34:8799–817.
[14] Nanda S, Li K, Abatzoglou N, Dalai AK, Kozinski JA. Advancements and confinements in hydrogen production technologies. In: Dalena F, Basile A, Rossi C, editors. Bioenergy systems for the future. UK: Woodhead Publishing, Elsevier; 2017. p. 373–418.
[15] Nanda S, Rana R, Hunter HN, Fang Z, Dalai AK, Kozinski JA. Hydrothermal catalytic processing of waste cooking oil for hydrogen-rich syngas production. Chem Eng Sci 2018;195:935–45.
[16] Kruse A, Krupka A, Schwarzkopf V, Gamard C, Henningsen T. Influence of proteins on the hydrothermal gasification and liquefaction of biomass. 1. Comparison of different feedstocks. Ind Eng Chem Res 2005;44:3013–20.
[17] Basu P, Mettanant V. Biomass gasification in supercritical water – a review. Int J Chem React Eng Rev 2009;7.
[18] Rana R, Nanda S, Maclennan A, Hu Y, Kozinski JA, Dalai AK. Comparative evaluation for catalytic gasification of petroleum coke and asphaltene in subcritical and supercritical water. J Energ Chem 2019;31:107–18.
[19] Kumar M, Oyedun AO, Kumar A. A review on the current status of various hydrothermal technologies on biomass feedstock. Renew Sustain Energy Rev 2018;81:1742–70.
[20] Xu X, Matsumura Y, Stenberg J, Antal MJ. Carbon-catalyzed gasification of organic feedstocks in supercritical water. Ind Eng Chem Res 1996;35:2522–30.
[21] Chakinala AG, Brilman DWF, Van Swaaij WPM, Kersten SRA. Catalytic and non-catalytic supercritical water gasification of microalgae and glycerol. Ind Eng Chem Res 2010;49:1113–22.
[22] Castello D, Kruse A, Fiori L. Low temperature supercritical water gasification of biomass constituents: glucose/phenol mixtures. Biomass Bioenergy 2015;73:84–94.
[23] Seif S, Tavakoli O, Fatemi S, Bahmanyar H. Subcritical water gasification of beet-based distillery wastewater for hydrogen production. J Supercrit Fluids 2015;104:212–20.
[24] Norouzi O, Safari F, Jafarian S, Tavasoli A, Karimi A. Hydrothermal gasification performance of *Enteromorpha intestinalis* as an algal biomass for hydrogen-rich gas production using Ru promoted Fe–Ni/γ-Al_2O_3 nanocatalysts. Energy Convers Manag 2017;141:63–71.
[25] Nanda S, Dalai AK, Kozinski JA. Supercritical water gasification of timothy grass as an energy crop in the presence of alkali carbonate and hydroxide catalysts. Biomass Bioenergy 2016;95:378–87.
[26] Nanda S, Reddy SN, Dalai AK, Kozinski JA. Subcritical and supercritical water gasification of lignocellulosic biomass impregnated with nickel nanocatalyst for hydrogen production. Int J Hydrogen Energy 2016;41:4907–21.
[27] Nanda S, Gong M, Hunter HN, Dalai AK, Gökalp I, Kozinski JA. An assessment of pinecone gasification in subcritical, near-critical and supercritical water. Fuel Process Technol 2017;168:84–96.
[28] Nanda S, Reddy SN, Vo DVN, Sahoo BN, Kozinski JA. Catalytic gasification of wheat straw in hot compressed (subcritical and supercritical) water for hydrogen production. Energ Sci Eng 2018;6:448–59.
[29] Castello D, Fiori L. Supercritical water gasification of biomass: thermodynamic constraints. Bioresour Technol 2011;102:7574–82.
[30] Loppinet-Serani A, Aymonier C, Cansell F. Supercritical water for environmental technologies. J Chem Technol Biotechnol 2010;85:583–9.
[31] Lee IG, Kim MS, Ihm SK. Gasification of glucose in supercritical water. Ind Eng Chem Res 2002;41:1182–8.
[32] Pińkowska H, Wolak P, Złocińska A. Hydrothermal decomposition of xylan as a model substance for plant biomass waste - hydrothermolysis in subcritical water. Biomass Bioenergy 2011;35:3902–12.
[33] Kang K, Azargohar R, Dalai AK, Wang H. Noncatalytic gasification of lignin in supercritical water using a batch reactor for hydrogen production: an experimental and modeling study. Energy Fuel 2015;29:1776–84.
[34] Nanda S, Reddy SN, Hunter HN, Dalai AK, Kozinski JA. Supercritical water gasification of fructose as a model compound for waste fruits and vegetables. J Supercrit Fluids 2015;104:112–21.
[35] Nanda S, Reddy SN, Hunter HN, Butler IS, Kozinski JA. Supercritical water gasification of lactose as a model compound for valorization of dairy industry effluents. Ind Eng Chem Res 2015;54:9296–306.

Please cite this article as: Okolie JA et al., Optimization and modeling of process parameters during hydrothermal gasification of biomass model compounds to generate hydrogen-rich gas products, International Journal of Hydrogen Energy, https://doi.org/10.1016/j.ijhydene.2019.05.132

[36] Yoshida T, Matsumura Y. Gasification of cellulose, xylan, and lignin mixtures in supercritical water. Ind Eng Chem Res 2001;40:5469–74.
[37] Muthukumar M, Mohan D, Rajendran M. Optimization of mix proportions of mineral aggregates using Box Behnken design of experiments. Cement Concr Compos 2003;25:751–8.
[38] Ferreira SLC, Bruns RE, Ferreira HS, Matos GD, David JM, Brandão GC, da Silva EGP, Portugal LA, dos Reis PS, Souza AS, dos Santos WNL. Box-Behnken design: an alternative for the optimization of analytical methods. Anal Chim Acta 2007;597:179–86.
[39] Yoshida T, Oshima Y, Matsumura Y. Gasification of biomass model compounds and real biomass in supercritical water. Biomass Bioenergy 2004;26:71–8.
[40] Lu YJ, Guo LJ, Ji CM, Zhang XM, Hao XH, Yan QH. Hydrogen production by biomass gasification in supercritical water: a parametric study. Int J Hydrogen Energy 2006;31:822–31.
[41] Ding N, Azargohar R, Dalai AK, Kozinski JA. Catalytic gasification of cellulose and pinewood to H_2 in supercritical water. Fuel 2014;118:416–25.
[42] Lv PM, Xiong ZH, Chang J, Wu CZ, Chen Y, Zhu JX. An experimental study on biomass air-steam gasification in a fluidized bed. Bioresour Technol 2004;95:95–101.
[43] Yetilmezsoy K, Demirel S, Vanderbei RJ. Response surface modeling of Pb(II) removal from aqueous solution by *Pistacia vera* L.: Box-Behnken experimental design. J Hazard Mater 2009;171:551–62.
[44] Rana R, Nanda S, Kozinski JA, Dalai AK. Investigating the applicability of Athabasca bitumen as a feedstock for hydrogen production through catalytic supercritical water gasification. J Environ Chem Eng 2018;6:182–9.
[45] Reddy SN, Nanda S, Dalai AK, Kozinski JA. Supercritical water gasification of biomass for hydrogen production. Int J Hydrogen Energy 2014;39:6912–26.
[46] Nanda S, Dalai AK, Gökalp I, Kozinski JA. Valorization of horse manure through catalytic supercritical water gasification. Waste Manag 2016;52:147–58.
[47] Swamy GJ, Sangamithra A, Chandrasekar V. Response surface modeling and process optimization of aqueous extraction of natural pigments from *Beta vulgaris* using Box-Behnken design of experiments. Dyes Pigments 2014;111:64–74.
[48] Dahmoune F, Spigno G, Moussi K, Remini H, Cherbal A, Madani K. *Pistacia lentiscus* leaves as a source of phenolic compounds: microwave-assisted extraction optimized and compared with ultrasound-assisted and conventional solvent extraction. Ind Crops Prod 2014;61:31–40.
[49] Soni SK, Goyal N, Gupta JK, Soni R. Enhanced production of α-amylase from *Bacillus subtilis* subsp. *spizizenii* in solid state fermentation by response surface methodology and its evaluation in the hydrolysis of raw potato starch. Starch 2012;64:64–77.
[50] Sadoun O, Rezgui F, G'Sell C. Optimization of valsartan encapsulation in biodegradables polyesters using Box-Behnken design. Mater Sci Eng C 2018;90:189–97.
[51] Toor SS, Rosendahl L, Rudolf A. Hydrothermal liquefaction of biomass: a review of subcritical water technologies. Energy 2011;36:2328–42.
[52] Gong M, Nanda S, Romero MJ, Zhu W, Kozinski JA. Subcritical and supercritical water gasification of humic acid as a model compound of humic substances in sewage sludge. J Supercrit Fluids 2017;119:130–8.
[53] Gong M, Nanda S, Hunter HN, Zhu W, Dalai AK, Kozinski JA. Lewis acid catalyzed gasification of humic acid in supercritical water. Catal Today 2017;291:13–23.
[54] Sivasangar S, Zainal Z, Salmiaton A, Taufiq-Yap YH. Supercritical water gasification of empty fruit bunches from oil palm for hydrogen production. Fuel 2015;143:563–9.
[55] Nanda S, Dalai AK, Berruti F, Kozinski JA. Biochar as an exceptional bioresource for energy, agronomy, carbon sequestration, activated carbon and specialty materials. Waste Biomass Valor 2016;7:201–35.
[56] Tiong L, Komiyama M, Uemura Y, Nguyen TT. Catalytic supercritical water gasification of microalgae: comparison of *Chlorella vulgaris* and *Scenedesmus quadricauda*. J Supercrit Fluids 2016;107:408–13.
[57] Samiee-Zafarghandi R, Karimi-Sabet J, Abdoli MA, Karbassi A. Supercritical water gasification of microalga *Chlorella* PTCC 6010 for hydrogen production: Box-Behnken optimization and evaluating catalytic effect of MnO_2/SiO_2 and NiO/SiO_2. Renew Energy 2018;126:189–201.
[58] Sinag A, Kruse A, Schwarzkopf V. Formation and degradation pathways of intermediate products formed during the hydropyrolysis of glucose as a model substance for wet biomass in a tubular reactor. Eng Life Sci 2003;3:469–73.
[59] Azadi P, Afif E, Azadi F, Farnood R. Screening of nickel catalysts for selective hydrogen production using supercritical water gasification of glucose. Green Chem 2012;14:1766–77.
[60] Yanik J, Ebale S, Kruse A, Saglam M, Yuksel M. Biomass gasification in supercritical water: Part 1. Effect of the nature of biomass. Fuel 2007;86:2410–5.
[61] Nanda S, Maley J, Kozinski JA, Dalai AK. Physico-chemical evolution in lignocellulosic feedstocks during hydrothermal pretreatment and delignification. J Biobased Mater Bioenergy 2015;9:295–308.
[62] Hu F, Ragauskas A. Pretreatment and lignocellulosic chemistry. Bioenerg Res 2012;5:1043–66.
[63] O'Sullivan AC. Cellulose: the structure slowly unravels. Cellulose 1997;4:173–207.
[64] Yang H, Yan R, Chen H, Lee DH, Zheng C. Characteristics of hemicellulose, cellulose and lignin pyrolysis. Fuel 2007;86:1781–8.
[65] Reddy SN, Nanda S, Hegde UG, Hicks MC, Kozinski JA. Ignition of *n*-propanol–air hydrothermal flames during supercritical water oxidation. Proc Combust Inst 2017;36:2503–11.
[66] Madenoğlu TG, Sağlam M, Yüksel M, Ballice L. Hydrothermal gasification of biomass model compounds (cellulose and lignin alkali) and model mixtures. J Supercrit Fluids 2016;115:79–85.
[67] Jarungthammachote S, Dutta A. Thermodynamic equilibrium model and second law analysis of a downdraft waste gasifier. Energy 2007;32:1660–9.
[68] Letellier S, Marias F, Cezac P, Serin JP. Gasification of aqueous biomass in supercritical water: a thermodynamic equilibrium analysis. J Supercrit Fluids 2010;51:353–61.
[69] Louw J, Schwarz CE, Knoetze JH, Burger AJ. Thermodynamic modeling of supercritical water gasification: investigating the effect of biomass composition to aid in the selection of appropriate feedstock material. Bioresour Technol 2015;174:11–23.

Please cite this article as: Okolie JA et al., Optimization and modeling of process parameters during hydrothermal gasification of biomass model compounds to generate hydrogen-rich gas products, International Journal of Hydrogen Energy, https://doi.org/10.1016/j.ijhydene.2019.05.132